doi:10.5937/jaes16-15905 Paper number: 16(2018)2, 521, 217 - 224

A CONTRIBUTION TO THE STUDY OF THERMAL LOADS OF HYDRAULIC AND ACTIVE MOUNTS OF POWERTRAIN OF A FREIGHT MOTOR VEHICLE

Miroslav Demić[1*] Đorđe Mihailo Diligenski[2]
[1]Engineering Academy of Serbia, Belgrade, Serbia
[2]University of Belgrade, Vinča Institute for Nuclear Science, Belgrade, Serbia

Due to the excitation from the road micro unevenness, powertrain vibration and conditions of motion (acceleration, braking, curved motion) trucks masses make complex spatial oscillatory movements. The negative impact of these movements, i.e. dynamic loads arising from those movements and transferred to the vehicle chassis, can be reduced by the proper choice of the position and characteristics of the powertrain mounts. The elastodamping forces in the mounts perform mechanical work which is converted into a thermal energy. Theoretical, experimental and combined methods can be used to analyse thermal loads of mounts. In this paper, research was carried out using theoretical methods using the simplified mechanical model of the powertrain. The vibrations of the powertrain of a trucks manufactured by FAP were observed. Thermal load analysis was performed for hydraulic and active mounts.

Key words: Truck, Powertrain, Vibration, Modelling

INTRODUCTION

As it is well known, vibration and noise are transferred from powertrain to chassis. In order to reduce this effect to a satisfactory level, powertrain is elastically linked to the vehicle chassis. This system simultaneously absorbs the vibrational excitation that, through the vehicle suspension system, is transferred to the powertrain. Due to the kinetic energy of the powertrain, arising from vibration, the mechanical work in mounts is converted into the heat energy [09].

In practice, the choice of characteristics of the powertrain suspension system is carried out from the conditions of good vibration damping that is transmitted from the vehicle chassis. However, thermal stresses that the powertrain mounts are exposed to are usually ignored, which, in cases of poor cooling, can cause degradation of their characteristics. Therefore, it is considered appropriate to analyse their thermal loads.

Research has shown that mechanical work due to the powertrain mounts vibrations turns into a heat transmitted, in a wider sense, to the environment [01, 03, 12, 16, 20]:

$$A = Q_t + Q_f + Q_o \tag{1}$$

where:

A -mechanical work (equivalent to the amount of heat),

Q_t - portion of heat transmitted to the mount body,

Q_f – portion of heat transmitted to the fluid (for hydraulic mounts), and

Q_o- portion of heat delivered to the environment.

The work of the forces in the mounts is important for the analysis of the thermal loads and it can be measured and experimentally measured with great difficulties [23-29]. Bearing in mind the distribution of heat inside the mount, as well as around it, the problem is significantly improved. It is noted that most of the heat is transferred by convection, and somewhat less by conduction and radiation [23]. Converting mechanical work into heat is much dependent on the mount design. Therefore, during the design of the powertrain suspension system, consideration should be given to creating conditions for good cooling. It is noted that the aim of this study was not to research the powertrain mounts cooling, but rather to determine the amount of heat generated by the vibrations in the mounts.

As it is known, classic supports consist of rubber-metal elements, with a damping effect coming from the rubber hysteresis. Hydraulic mounts have additional damping effect of the oil flow inside the mount. Bearing in mind the representation of classic - mechanical and hydraulic powertrain mounts in modern freight vehicles, the paper analyses mount thermal loads of a vehicle from the production program of the manufacturer FAP [11].

Motor vehicles represent complex vibrational systems with a majority of masses interconnected by elasto-damping elements, usually of non-linear characteristics. When traveling on uneven roads, and also due to the impact of the excitations coming from the engine and rotating elements, the vehicle performs random spatial vibratory movements. The negative impact of vibration on the characteristics of motor vehicles can be reduced by the correct selection of the position and characteristics of the elasto-damping elements. This can be done using theoretical-experimental, theoretical or experimental methods [04 - 06, 08, 09, 13, 14, 17, 18].

In the literature [04 - 06, 8, 9, 13, 14, 17, 18], a number of mathematical-experimental procedures for modelling of the behaviour of the powertrain are described. In this

* *University of Belgrade, Vinča Institute for Nuclear Science, 12-14 Mike Petrovića Street, Belgrade, diligens@vinca.rs*

paper, a medium payload truck FAP 1213 was observed, whose diagram of the powertrain suspension is shown in Figure 1, and the model relies on the procedure based on the principles of classical mechanics [22].

MODEL OF THE POWERTRAIN

Depending on the task being handled, various mechanical models of the powertrain and vehicles can be found. It is known from [04 - 06, 8, 9, 13, 14, 17, 18] that in the course of the analysis of the problem of transmission of dynamical loads from the powertrain to the frame of the vehicle, the cabin vibration and the cargo box can be neglected. More precisely, the analysis includes only the vibratory movement of the vehicle powertrain and the corresponding excitation from the vehicle frame.

The general rule in modelling mechanical systems, and in this case powertrain vibration, is to select the model structure so that it includes the minimum number of parameters that allows the analysis of the desired variable. This points out the need to use as simple as possible mathematical models, because due to the lack of precise inertial parameters of the powertrain, as well as the mount characteristics, more complex models can lead to larger errors [05, 06, 08, 09]. In this case, the layout of powertrain suspension of the observed freight vehicle FAP 1213 is shown in Figure 1.

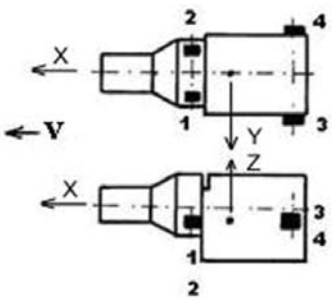

Figure 1: Scheme of powertrain suspension of the observed freight vehicle

Powertrain, as a solid body in the space, has six degrees of motion freedom (three translations and three rotations) [13, 22, 24]. Geometric C.G. axes have been adopted here so as to observe the motion of the powertrain, starting in an equilibrium position, which will be discussed later. It is important to note that the use of geometric axes leads to the need for the use of centrifugal moments of inertia, but, in light of the easier analysis, it is considered necessary to introduce the assumption that they are at the same time the main axes of inertia. Powertrain performs spatial vibrations under the influence of excitations received from the frame (which arise from the unevenness of the road and the vibration of the frame as an elastic system), as well as from the inertial forces and torque of the engine and rotating masses, and the like.

In order to describe the vibrational motion of the powertrain, we will adopt two coordinate systems, [22, 24], Figure 2:

- fixed and
- mobile, which is firmly attached to the powertrain.

The motion of the powertrain C.G. in the space is defined by the coordinate Z and the rotation of the powertrain around the C.G. (as a fixed point) is described by the angle φ - roll.

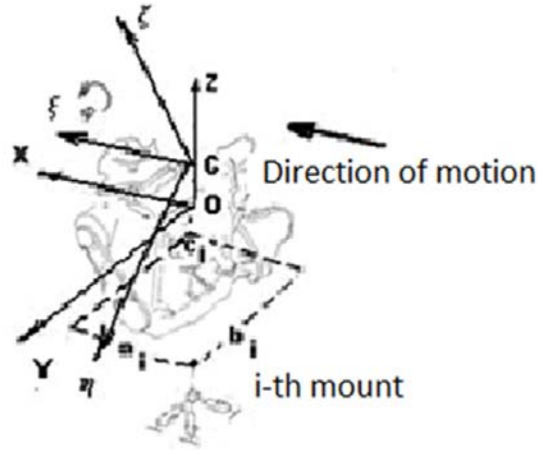

Figure 2: Introduced coordinate system to describe motion of the powertrain

To describe spatial motion of the powertrain, Newton-Euler equations were used [22].

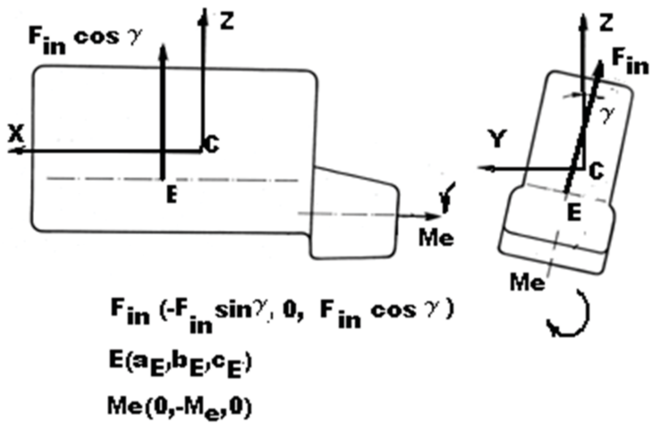

Figure 3: Excitations due to inertial forces and engine torque

Legend:

F_{in} - resulting inertial force of the piston group

M_e - engine torque

E - Acting point of the resulting inertial force and its coordinates relative to the moving coordinate system

y - angle of powertrain inclination (in this case, 0 °)

$$M\,\ddot{Z}_C = \sum Z_i \qquad 2)$$

$$I_u\,\ddot{\varphi} = \sum M_F \qquad 3)$$

In the literature [04, 05, 06, 08, 09, 13-15, 17, 18, 21, 23-29], there is a large number of mathematical models of the powertrain mounts, which are essentially more or less complicated (different structures). Some of them include fluid flow within the mounts, which is a rather complex problem. Bearing in mind that in this work the goal was to compare thermal loads of the mount in a comparative study, it was considered appropriate that the simpler terms should be used for the approximation of forces in the mounts.

Forces in the elastic mount [05]:

$$F_{ci} = c_{i1}\,\Delta_i + c_{i2}\,\Delta^2 + c_{i3}\,\Delta^3 \qquad 4)$$

where:

c_i, c_{i1}, c_{i2}, c_{i3} - stiffness coefficients,

Δ - relative deformation of the mount.

Damping forces in the mounts are assumed in the form [05].

$$F_{ai} = k_{i1}\,\dot{\Delta} + k_{i2}\,\dot{\Delta}^2\, sign(\dot{\Delta}) \qquad 5)$$

where:

k_{i1}, k_{i2}- damping coefficients,

$\dot{\Delta}$ - relative velocity of mount deformation, and

sign – mathematical function.

Deformations and deformation velocities of the powertrain mounts are defined by the following expressions (Figure 2):

$$\Delta = Z - Z_O - b_i(\varphi - \varphi_O) \qquad 6)$$

$$\dot{\Delta} = \dot{Z} - \dot{Z}_O - b_i(\dot{\varphi} - \dot{\varphi}_O) \qquad 7)$$

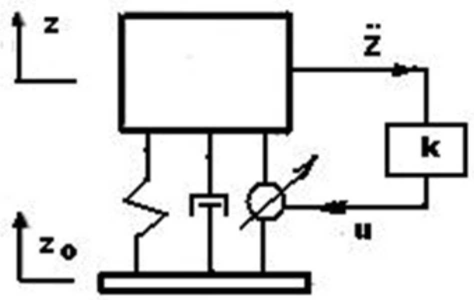

Figure 4: Block scheme of hydraulic and active mount

In order to analyse the influence of the active suspension system of the powertrain, it is assumed that on each support there is an actuator whose direction of force coincides with the axis Z. It will be assumed that this function is the absolute acceleration in the direction of Z axis [05], Figure 4:

$$F_a = -k\; acc_i \qquad 8)$$

where:

acc=d[9]+bd[10] - measured acceleration of each mount,

k – feedback amplification.

In this case, a four-stroke four-cylinder in-line diesel engine with a crankshaft whose cranks are in the same plane (180 ° angle) was used. In the piston mechanisms, there are forces [19], that drive piston (the forces of gases and the inertial force of the piston group), and on the movable bearing of the crank, the centrifugal and tangential force of the crankshaft occur. In balancing the inertial forces of the piston group mass (ideally if the force develops into the Fourier series), there remain unbalanced inertial forces of the second and higher orders. It is noted that when there are differences in the of piston group masses per cylinders, the unbalanced forces of the first order are also present (in this specific case, the the masses were equal).

Assuming that higher-order harmonics can be neglected, the unbalanced inertial force of the observed engine can be expressed in the form [19].

$$F_{in} = 4\, m_r \cdot \omega^2 \cdot \lambda \cdot \cos 2\omega t \qquad 9)$$

where:

m_r - is reduced mass of the piston group,

r - radius of the crankshaft crank,

ω - angular speed of the engine crankshaft,

λ - ratio of the radius of the crankshaft krank and the length of the piston rod,

t - time.

Using elementary knowledge from the vector theory and principles of statics, and taking into account Figures 2 and 3, the moment from the resulting inertial force is defined by the expression (9) [05] is:

$$\vec{M}_{Fin} = \begin{bmatrix} \overrightarrow{u_0} & \overrightarrow{v_0} & \overrightarrow{w_0} \\ a_E & b_E & c_E \\ -F_{in}\sin\gamma & 0 & F_{in}\cos\gamma \end{bmatrix} \qquad 10)$$

where values in the expression (10) correlate with the Figure 3.

Centrifugal forces are partially counterbalanced by counter weights, or other procedures, which will not be discussed here [19].

Tensile force causes the torque of the engine, which due to its variation has a variable value (unevenness is partially reduced by the flywheel) [19].

In the absence of precise data, it is assumed that the torque that affects the powertrain can be described by the following equation [05]:

$$M = -M_e \cdot i_0 \cdot i_m (0{,}95 + 0{,}1 \cdot rnd) \qquad 11)$$

where:

M_e - engine torque,

i_0 – rear axle ratio,

i_m – transmission ratio,

r_{nd} - random numbers evenly distributed within the interval [0,1].

Vibration of the powertrain is also influenced by the vibration of the vehicle frame, which are of random character [5, 13, 24]. Bearing in mind that the complexity of the vehicle spatial model exceeds the needs of this paper, it is considered appropriate that in this specific case the excitations coming from the frame and obtained on the basis

excitation = max (r_{nd} – 0.5) 12)

of the model should not be used. Instead, the broadband functions of the excitation have been adopted:

where,

max = 0.01m, rad,

r_{nd} – the same meaning already mentioned with the engine torque.

Projections of the generalized forces include all components of the forces and torques of the corresponding mounts in the direction of the observed axis (for mounts 1 to 4), inertial forces and moments of the engine torque, and the unbalanced inertial forces and forces of the active suspension.

THERMAL LOADS OF THE POWERTRAIN MOUNTS

Due to the relative motion of the powertrain and vehicle frame, the work is carried out in the mounts, which is

$$A=\int_0^s F_m dz_{rel}=\int_0^T F_m \dot{z}_{rel} dt \quad 13)$$

equivalent to the amount of heat Q [01, 03, 09, 12, 16]. The mechanical work in the mount is defined by the expression [01, 03, 09, 12, 16]:

where:

F_m – elastodamping forces in the mount,

z_{rel} $\dot{z}_{rel}$ - relative deformation and speed of mount deformation (respectively), and

$$P=\frac{A}{T}=\frac{k}{T}\int_0^T \dot{z}_{rel}\, dt \quad 14)$$

t – time.

$$\dot{z}_{relef}^{\,2}=\frac{1}{T}\int_0^T \dot{z}_{rel} dt \quad 15)$$

Mean power is given by expression:

$$P=k\,\dot{z}_{relef}^{\,2} \quad 16)$$

Since the effective value of the relative speed is:

the mean power can be written in the following form:

$$P=\alpha S\Delta\tau \quad 17)$$

Mean power is transformed into heat, with the dominant αnvection:

where:

$\Delta\tau$- heat transition coefficient,

S – area of convection, and

- teαperature difference between the mount and environment

Since $_i$ and S_i are unknown values, whose definition requires highly complex research, this will not be discussed in this paper.

Bearing in mind that all four mounts had the same characteristics, it was considered appropriate to carry out an analysis of summarized thermal loads.

NUMERICAL SIMULATION AND ANALYSIS OF THE REULTS

On the basis of the expressions (2-16), it can be noticed that differential equations describing the spatial vibrations of the vehicle powertrain are non-linear, it was necessary to solve them numerically by use of the Runge-Kuta method. The integration was carried out with the time increment of 0.0001 s, in 524288 points. This enabled a reliable analysis within the range 0.019-5000 Hz. It is obvious that this range is considerably broader than the excitation range of engine and the complete vehicle powertrain. The integration of differential equations is performed for the cases of classical and hydraulic mounts.

More precise analyses related to errors in the calculation of spectra [02] show that for the desired relative random error of 0.1, the relative bias error 0.02, the coherence between the input and the output value of 0.85, it is necessary to make 100 averagings for calculating the autospectra and 138 averagings for calculating of cross-spectra. Since the applied software [10] carried out 2048 aaveragings, it is obvious that errors in the calculation of spectra were made significantly below the upper limits permitted by the technical systems [02, 07, 10].

The parameters of the observed vehicle and its pow-

Table 1: Characteristic parameters of the vehicle FAP 1213 and its powertrain

Maximum engine power, kw	100
Maximum engine speed, min^{-1}	2600
Maximum engine torque, Nm	428
Speed at maximum torque, min^{-1}	1300
Vehicle weight, kg	12000
Powertrain weight, kg	1680
Moments of inertia Ix/Iy/Iz, kgm^2	85/35/72
Rear axle ratio, -	3.83
Transmission ratio in direct gear, -	1

Table 2: Coordinates of the mount attachments

Position of mounts	a, m	b, m	c, m
Mount 1	0.5	0.4	0.1
Mount 2	0.5	-0.4	0.1
Mount 3	-0.5	0.4	0.1
Mount 4	-0.5	-0.4	0.1

ertrain are given in Table 1, and the coordinates of the points of attachment (mounts) in Table 2.

Stiffness of the hydraulic mounts in direction of axes X, Y and Z, which were experimentaly determined by FAP, are shown in the Table 3.

Table 3: Stiffness of the used hydraulic mounts

	c_{i1}, N/m	c_{i2}, N/m^2	c_{i3}, N/m^3
X	1200000	250000	60000
Y	1200000	250000	60000
Z	1200000	250000	60000

In the absence of more precise data, the damping characteristics of the hydraulic mounts are roughly defined on the basis of the mount stiffness and the weight they carry [05], and are given in Table 4.

Table 4: Presumed damping characteristics of the mounts

	k_{i1}, Ns/m	k_{i2}, Ns^2/m
X	62000	100
Y	62000	100
Z	62000	100

In the absence of more precise data, the value of the feedback amplification in the case of active mounts was adopted to be 100.

For the sake of illustration, the vertical vibration excitations of the powertrain as a result of frame excitation are shown in Figure 5. It is obvious that the excitations are very variable and so it is necessary to expect significant heat loads of the powertrain mounts. A similar observation also applies when it comes to the excitations of frame roll, which are not shown here.

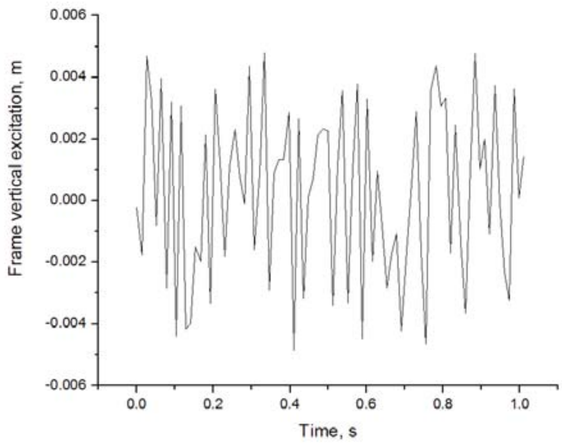

Figure 5: Illustration of the frame vertical excitation

Summarized thermal loads (for all components of forces and torques, for all four mounts) are calculated using the expressions (2-16), and the results are shown in Figure 6.

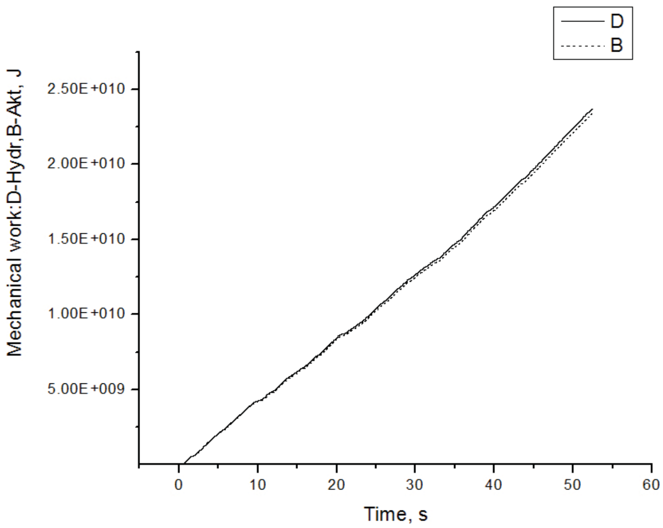

Figure 6: Amount of heat (mechanical work) depending on the type of mount

The analysis of the Figure 6 shows that hydraulic mounts bear a slightly higher thermal load than the active ones (for 52 s, hydraulic approx. 2.373 1010 J, and active approx. 2.342 1010 J). Figure 6 shows that the amount

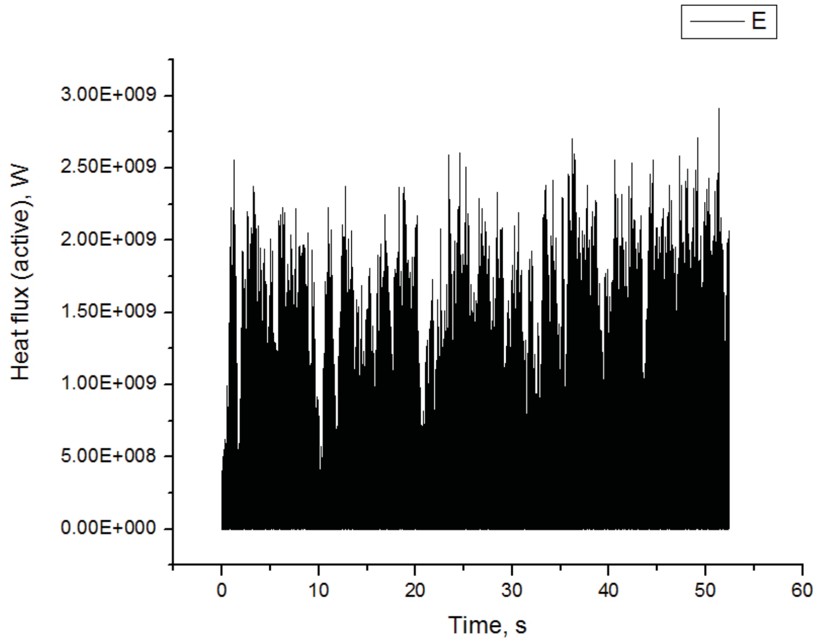

Figure 7: Heat flux of the active mounts

of heat increases with time, and that in the absence of cooling, they would experience degradation of the shape and characteristics.

As noted above, the heat flux for both types of mounts is calculated, and for the illustration in Figure 7, the flux for active mounts is shown. It is obvious that it varies in stochastic manner with time, so it is useful to calculate the effective values for the both types of mounts, which are given in the Table 5.

Table 5: RMS of heat flux

Mounts	RMS, W
Hydraulic	580791310.40
Active	572616837.05

The analysis of the data from the Table 5 shows that the thermal flux is somewhat lower in the active mounts compared to the hydraulic ones. It is noted that the performed research was aimed at determining the ratio of thermal loads of classical and hydraulic mounts, using the model, so that the obtained results can be adopted as orientational, which is acceptable at the stage of development of the conceptual design of a freight motor vehicle.

As the purpose of the research was to determine which component of the excitation (including engine excitation forces and torques) has the major influence on the thermal load of the powertrain mounts, it is estimated to be worthwhile to clarify this problem in more detail. It is known that a dynamic system with multiple input variables and one output variable can be shown in Figure 8 [02, 07, 10]. In case that there is a connection between the input variables, the system must first decouple [02, 07, 10]. As in our case this is a system whose heat loads depend on 4 excitations (2 displacements, and two excitations from the engine), we will summarize the theory that allows the analysis of

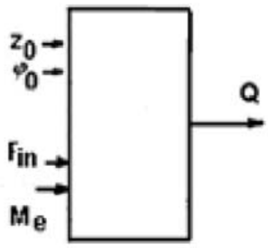

Q - amount of heat or heat flux,
z_0 - frame vertical excitation (x_1),
φ_0 frame roll excitation (x_2),
F_{in} – engine inertial force of the second order (x_3),
M_e- engine torque (x_4)

Figure 8: Block scheme of the powertrain suspension

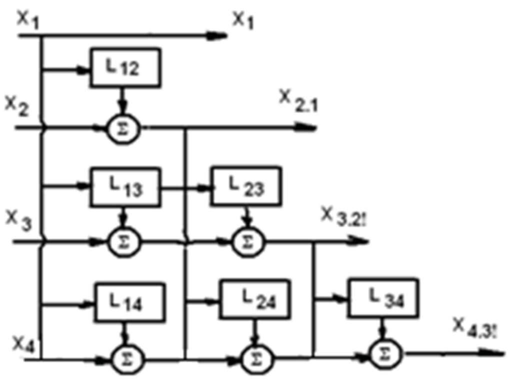

Figure 9: Decoupling scheme

the impact of each individual excitation on the thermal load of the powertrain mounts, in particular, the heat flux. Figure 9 shows the decoupling scheme [02, 10].

$$
\begin{aligned}
&x_{1!} = x_1\,, \\
&x_{2\cdot1!} = x_1 - L_{12}\cdot x_1\,, \\
&x_{3\cdot2!} = x_3 - L_{13}\cdot x_1 - L_{23}\cdot x_{2\cdot1!}\,, \\
&x_{4\cdot3!} = x_4 - L_{1\cdot4}\cdot x_1 - I_{2\cdot1}.x_{2\cdot4!} - L_{3\cdot4}\cdot x_{3\cdot2!}
\end{aligned}
\qquad 18)
$$

Bearing in mind the theory from [2] and Figure 8, the following can be written (all variables are given in the complex plane - Fourier or Laplace transformation):

where

x_1, x_2, x_3, x_4 – input variables,

$x_{21!}$, $x_{32!}$, $x_{43!}$ - second conditional input with eliminated influence of the first input; the third conditional input with the elimination effect of the first and second conditional inputs; the fourth conditional input with the elimination of the influence of the first and conditional second and third

$$L_{12} = \frac{x_2}{x_1} \quad L_{13} = \frac{x_3}{x_1} \quad L_{14} = \frac{x_4}{x_1}$$
$$L_{23} = \frac{x_{3\cdot 2!}}{x_{2\cdot 1!}} \quad L_{24} = \frac{x_{4\cdot 3!}}{x_{2\cdot 1!}} \qquad 19)$$

conditional inputs, respectively.

The transfer functions between the input variables can be displayed as follows:

where L_{12}, L_{13}, L_{14}, L_{23}, L_{24} are the corresponding transfer functions between the conditional input variables.

Note that transfer functions indicate how much output variable is amplifying or weakening in relation to the in-

$$\gamma_{iQ(i1)!}^{\;2} = \frac{\left[S_{iQ(i-1)!}\right]^2}{S_{xx(i-1)!}S_{QQ(i-1)!}} \qquad 20)$$

put variable, and how much is the phase delay between them. On the basis of expressions (18, 19), partial coherence functions can be calculated, which indicate the coupling between input and output signals [02].

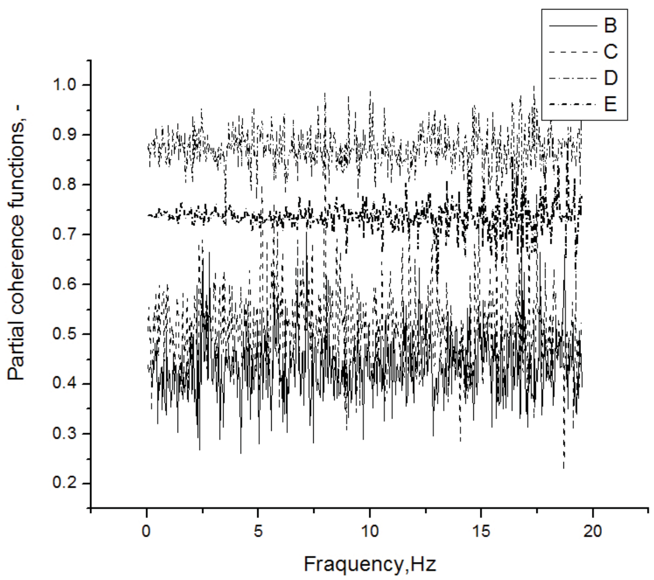

Figure 10: Partial coherence functions for active mounts: B - frame vertical excitations, C – frame roll excitation with the excluded effect of vertical excitation, D - inertial force with the excluded impact of the frame vertical and roll excitation, and E – engine torque with the excluded influence of frame vertical and roll excitation and the inertial force of the engine

where:

- $S_{iQ(i-1)!}$ – crosspectrum, and
- $S_{xx(i-1)!}$ and $S_{QQ(i-1)!}$ – corresponding autospectra [02].

For the purpose of a more detailed analysis, partial coherence functions are calculated (expression 20), and for the purpose of illustration in Figure 10, calculated values for active mounts are shown. Data analysis for hydraulic and active mounts, given in Figure 10, shows that partial coherent functions depend on frequency and type of excitation. It is considered worthwhile to conduct a more

Table 6: Minimum, maximum and RMS values of partial coherence functions for hydraulic mounts

	min.	max.	RMS
B	0.252	0.741	0.448
C	0.216	0.897	0.506
D	0.721	1.000	0.873
E	0.600	0.839	0.711

Table 7: Minimum, maximum, and RMS values of partial coherence functions for active mounts

	min.	max.	RMS
B	0.261	0.731	0.442
C	0.227	0.938	0.518
D	0.720	1.000	0.874
E	0.606	0.883	0.737

detailed analysis of data on partial coherence functions. In this sense, the minimum, maximum and effective values of the partial coherent functions are calculated and given in Tables 6 and 7.

Analysis of the data from the above tables shows that the type of mounts has an influence on the partial coherence functions, and that their values are within the interval of 0.216 to 1, indicating that there is a coupling between the input variables and the heat flux [02]. The analysis of the effective values shows that the inertial force and the engine torque have a greater impact on the thermal loads of the mounts.

The performed research was aimed at determining the relationship of thermal loads of hydraulic and active mounts, by use of models, so the obtained results can be adopted as orientational, which is necessary in the design phase of the conceptual design of a freight motor vehicle.

CONCLUSIONS

Based on the performed research, it can be concluded that the applied model of the powertrain can be used to simulate thermal loads of the powertrain mounts of trucks. The performed analyzes have shown that the active mounts have a somewhat lower thermal load than hydraulic mounts of powertrain.

REFERENCES

1. Atkins, P. (2010). The Laws of Thermodynamics (A Very Short Introduction). Oxford.
2. Bendat J.S., Piersol A.G. (2000) Random Data-Analysis and measurement procedures. London: John Wiley and Sons.
3. Bojić, M. (2011). Thermodynamics (in Serbian). University of Kragujevac, Mechanical Engineering Faculty.
4. Catalin, A., Aleksandru, P. (2011). A comparative analysis between the vehicles passive and active suspensions. International Journal of Mechanics, Issue 4, Vol. 5, 371-378.
5. Demić, M. (1990). A contribution to the optimization of the position and the characteristics of passenger cars powertrain mounts. Int. J. of Vehicle Design, Vol. 1, No 1, 87-103.
6. Demić, M. (1997). Identification of Vibration Parameters for Motor Vehicles. Vehicle System Dynamics, Vol. 27, 65-88.
7. Demić, M. (2003). ANALSIGDEM: Software for signal analysis.
8. Demić, M. (1997). The Optimization of Vibratory Systems of Motor Vehicles (monograph, in Serbian). Mechanical Engineering Faculty, Kragujevac.
9. Demić, M., Diligenski, Đ. (2016). Numerical simulation of shock absorbers heat load for semi-active suspension system, Thermal of science, doi: 10.2298/TSCI150624005D, 1-17.
10. Demić, M. (2003). DEMPARCOH: Softwares for signal analysis.
11. FAP Information (2017).
12. Fermi, E. (2011). Thermodynamics. Dover Books on Physics.
13. Genta, A. (2003). Motor Vehicle Dynamics, Politecnika di Torino.
14. Gowda, D. Chacrasaly, S. (2014). Comparative Analysis of Passive and Semi-active Suspension System for Quarter Car Model using PID Controller. Association of Computer Electronics and Electrical Engineers, DOI 03.AETS.2014.5.131.
15. Igami, H., Thompson, M., and Osodo, K. (2008). Automotive Powertrain Mounting System Design Optimization. SAE Technical Paper 2008-01-0879, doi:10.4271/2008-01-0879.
16. Ilić, G., et al. (1996). Thermodynamics II, Basics of heat transfer (in Serbian), University of Niš, Mechanical Engineering Faculty.
17. Kennings, P., Layfield, J., Tarabra, M., Fothergill, D., Syred, F., Franks, G. (2014). Developing Powertrain Mounting Systems in the Virtual Engineering World Using a Full Vehicle NVH Simulator. InterNoice, Melbourne, Australia, 16-19 November, 1-10.
18. Liu, X., Lv, Z., and Shangguan, W. (2015). Design of Powertrain Mounting System for Engine with Three Cylinders. SAE Technical Paper 2015-01-2354, doi:10.4271/2015-01-2354.
19. Mahalec, I. et al. (2015). Konstrukcije motora, FSB, Zagreb.
20. Moran, MJ., et al. (2010). Fundamentals of Engineering Thermodynamics, Wiley.
21. Park, J., Singh, R. (2009). Analysis of powertrain motions given a combination of active and passive isolators. Noise Control Eng. Vol. 57, 232-243.
22. Pars, L. (1971). A Treatise on Analytic Dynamics, Heinemann, London.
23. Qingzheng, W, N., Wang, N.(2016). Automotive Powertrain Mounting System Optimum Design and Simulation Analysis. Proceedings of the 2011 IAJC-ASEE International Conference ISBN 978-1-60643-379-9, 1-14.
24. Simić, D., Demić, M. (1992). Mounting of the power train (monograph), MVM.
25. Shanguan, W., Liu, X., Lv, Z., Rakheja, S. (2016). Design Method of automotive powertrain mounting system based on vibration and noise limitations of vehicle level. Mechanical Systems and Signal Processing, Elsevier Ltd, 677-695.
26. Sui, J., Hoppe, C., Hirshey, J. (2003). Powertrain Mounting Design Principles to Achieve Optimum Vibration Isolation with Demonstration Tools. SAE Technical Paper 2003-01-1476, doi:10.4271/2003-01-1476.
27. Turnip, A., Hong, K., Park, S. (2009). Modelling of a hydraulic engine mount for active pneumatic engine vibration control using the extended Kalman filter. Journal of Mechanical Sciences and Technology, 23, 229-236.
28. When, B.S, Xiao, P, L., Zhao, P.L, Subash, R. (2016). Design method of automotive powertrain mounting system based on vibration and noise limitations of vehicle level. Mechanical System and Signal processing, Vol. 76-77, 677-695.
29. Wen-Bin Shanguan, et al. (2016). Design method of automotive powertrain mounting system based on vibration and noise limitations of vehicle level. Mechanical Systems and Signal Processing, 677-695.

Paper submitted: 04.12.2017.
Paper accepted: 22.01.2018.